

CD8⁺ T Cells in Facioscapulohumeral Muscular Dystrophy Patients with Inflammatory Features at Muscle MRI

Giovanni Frisullo · Roberto Frusciante · Viviana Nociti · Giorgio Tasca ·
Rosaria Renna · Raffaele Iorio · Agata Katia Patanella · Elisabetta Iannaccone ·
Alessandro Marti · Monica Rossi · Assunta Bianco · Mauro Monforte ·
Pietro Attilio Tonali · Massimiliano Mirabella · Anna Paola Batocchi · Enzo Ricci

Received: 29 August 2010 / Accepted: 28 September 2010 / Published online: 10 November 2010
© Springer Science+Business Media, LLC 2010

Abstract Facioscapulohumeral muscular dystrophy (FSHD) is an inherited disease, and although strongly suggested, a contribution of inflammation to its pathogenesis has never been demonstrated. In FSHD patients, we found by immunohistochemistry inflammatory infiltrates mainly composed by CD8⁺ T cells in muscles showing hyperintensity features on T2-weighted short tau inversion recovery magnetic resonance imaging (T2-STIR-MRI) sequences. Therefore, we evaluated the presence of circulating activated immune cells and the production of cytokines in patients with or without muscles showing hyperintensity features on T2-STIR-MRI sequences and from controls. FSHD patients displaying hyperintensity features in one or more muscles showed higher CD8⁺pSTAT1⁺, CD8⁺T-bet⁺ T cells and CD14⁺pSTAT1⁺, CD14⁺T-bet⁺ cells percentages and IL12p40, IFN γ and TNF α levels than patients without muscles displaying hyperintense features and controls. Moreover, the percentages of CD8⁺pSTAT1⁺, CD8⁺T-bet⁺ and CD14⁺pSTAT1⁺ cells correlated with the proportion of muscles displaying hyperintensity features at T2-STIR sequences. These data

indicate that circulating activated immune cells, mainly CD8⁺ T cells, may favour FSHD progression by promoting active phases of muscle inflammation.

Keywords T-bet · pSTAT1 · cytokines · FSHD · muscle MRI · CD8 T cells · inflammation

Introduction

Tissue damage in genetic disorders leads to the release of intracellular proteins and possibly the breakdown of tolerance, which can result in autoimmunity. The subsequent chronic autoimmune damage results in increased tissue degeneration [1] as observed in Duchenne muscular dystrophy, X-linked adrenoleukodystrophy and alpha 1-antitrypsin deficiency, in which a contribute of autoimmunity to the tissue damage has been demonstrated [2–5]. Moreover, in limb girdle muscular dystrophy (LGMD) type 2B and Miyoshi myopathy, dysferlin deficiency besides inducing muscle fibre degeneration can “per se” directly activate monocytes leading to an enhanced phagocytosis of damaged myofibres [6]. Facioscapulohumeral muscular dystrophy (FSHD) is an autosomal dominant inherited myopathy that is not due to mutation within a protein-coding gene but, in more than 95% of cases, is associated with a low number of 3.3-kb tandem repeat units, termed D4Z4, located on chromosome 4q35 [7]. To date, no causal gene has been identified, and epigenetic mechanisms that determine the loss of appropriate gene expression control seem to be involved in the pathogenesis of disease [8, 9]. Although a reliable genetic test is available for diagnostic purposes, very little is still known about the molecular mechanisms that induce muscle degeneration. Early studies focused on the presence of inflammatory features at

G. Frisullo · R. Frusciante · V. Nociti · G. Tasca · R. Renna ·
R. Iorio · A. K. Patanella · E. Iannaccone · A. Marti · M. Rossi ·
A. Bianco · M. Monforte · P. A. Tonali · M. Mirabella ·
A. P. Batocchi (✉) · E. Ricci
Institute of Neurology, Department of Neurosciences,
Catholic University of Rome,
largo Gemelli 8,
00168 Rome, Italy
e-mail: annapaola.batocchi@rm.unicatt.it

V. Nociti · A. K. Patanella · M. Rossi · P. A. Tonali ·
M. Mirabella · E. Ricci
Fondazione Don Carlo Gnocchi,
Via Capecelatro 66,
20148 Milan, Italy

histochemical muscle biopsy examination in many FSHD patients [10–12]. However, a 3-month prednisone pilot trial failed to show improvement in strength or muscle mass [13], and a pathogenic role for immunity has never been demonstrated. Magnetic resonance imaging (MRI) is emerging as a powerful tool in clinical practice to assess severity, distribution and characteristics of muscle involvement in muscular disorders, including FSHD [14–17]. Indeed, T1-weighted (T1-W) sequences are able to detect features of replacement of muscle with fibrosis or adipose tissue, while hyperintensity features at muscle MRI T2-weighted short tau inversion recovery (T2-STIR) sequences reflect changes in tissue water distribution and have been described in disorders characterized by oedema and inflammation or by denervation atrophy [18, 19]. Recently, we studied pelvic and lower limb muscles in FSHD patients by means of muscle MRI and observed, besides features of muscle tissue replacement on T1-W sequences, single or multiple focal areas of signal hyperintensity on T2-STIR sequences in 121 out of 202 patients (60%; unpublished data). As we hypothesized that these areas may represent features of muscle inflammation, in this study we performed immunohistochemistry on biopsies from FSHD patients obtained from muscles either or not showing hyperintensity features on T2-STIR sequences at MRI. Moreover, since the analysis of cytokines and cytokine induced transcription factors expressed in peripheral blood mononuclear cells (PBMC) may contribute to a better understanding of the pathophysiological mechanisms underlying inflammatory/autoimmune processes, we evaluated the presence of activated immune cells in the peripheral blood of FSHD patients and controls assessing the percentages of circulating CD4⁺, CD8⁺ and CD14⁺ cells positive for the transcription factors T-bet and pSTAT1, master regulators of Th 1 cells and pSTAT3, involved in the differentiation of Th17 cells. Finally, we measured the spontaneous production of several pro-inflammatory (IL12/IL23p40, IL6, IFN γ , IL17, TNF α) and anti-inflammatory cytokines (IL10 and TGF β) by cultured PBMC from FSHD patients and healthy subjects.

Materials and Methods

Patients and Controls

Patients with a genetically confirmed diagnosis of FSHD (pathogenic EcoRI/BlnI-resistant fragment ranging between 10 and 40 kb) and sex- and age-matched healthy subjects were screened for infectious conditions or other inflammatory diseases and then included in our study. Clinical examination and muscle MRI were performed in all patients before the inclusion in the study. Clinical severity

was assessed by a 10-grade Clinical Severity Scale (CSS) [20] assigning a score to the overall level of mobility limitations (from 0.5=facial weakness to 5=wheelchair bounded); according to this scale, higher scores (3 to 5) are assigned to patients with pelvic and proximal lower limb muscle involvement. None of the patients was under pharmacological treatments at the time of the study. This study was approved by the local ethics committee, and all the participants gave written informed consent before enrolment according to the Declaration of Helsinki [21].

MRI Protocol

Muscle imaging was performed on a 1.5-T MR scanner. Participants were examined by T1-W spin echo (TR/TE=500/35 ms) and T2-STIR (T1=150 ms) sequences. Ten-millimetre contiguous axial slices were obtained from the proximal lumbar spine to the ankles according to a protocol commonly used in the assessment of muscle disorders [16]. A total of 37 muscles on each body side were independently and blindly evaluated by two investigators (ER and RF) who had been extensively trained in muscle MRI evaluation.

According to T1-W sequences, each muscle was scored 0 (normal) to 4 (end-stage appearance, whole muscle replacement by connective tissue and fat) as reported [14]. As an index of disease severity, a T1 MRI score was obtained for each patient by summing all the single muscle scores.

Each muscle showing hyperintensity features on T2-STIR sequences was rated 1. A T2-STIR-MRI score corresponded to the number of such muscles observed in each patient.

On the basis of T2-STIR sequences, we split the patients into two groups: Group 1 included all individuals who showed no hyperintensity features (T2-STIR-MRI score=0); group 2 included all individuals displaying hyperintensity features (T2-STIR-MRI score >0). It is worth noting that the T1 MRI score, indicating the overall severity and extension of irreversible muscle fatty-fibrous replacement, did not have any influence on patient group assignment. Interobserver reliability was tested on all muscle MRI examinations. To test intraobserver reliability, muscle MRI of all FSHD patients were evaluated twice by each investigator with a 30-day period interval. A good sampled data reproducibility (<3% changes for the 1,850 evaluated muscles in both T1- and T2-STIR-W sequences) was obtained in both cases.

Immunohistochemistry

Biopsy was performed on five muscles showing hyperintensity features on T2-STIR sequences at MRI and on

five muscles with no hyperintensity features on T2-STIR sequences. All biopsies were obtained after written informed consent.

Immunohistochemistry was performed on 6- μ m cryostat sections using the following primary antibodies from Dako (Carpinteria, CA, USA): monoclonal mouse anti-human CD8, CD4, HLA ABC, HLA DP, DQ, DR, CD68, C5bC9 (MAC) and CD20; monoclonal mouse anti-human CD138 was purchased from Serotec (Raleigh, NC, USA) and monoclonal mouse anti-human perforin 1 (1.VB.3) from Santa Cruz Biotechnology (Santa Cruz, CA, USA). Muscle fibres were counterstained with FITC-conjugated phalloidin, and nuclei were visualized with Hoechst 33258 (Molecular Probes Inc.) staining. Sections were analysed using TCS SP5 laser scanning confocal microscope (Leica Microsystems, Wetzlar, Germany).

Isolation of Peripheral Blood Mononuclear Cells

PBMC were isolated from venous blood by density gradient centrifugation (2,500 rpm, 30 min) over a Ficoll-Hypaque density gradient (Pharmacia, Uppsala, Sweden). PBMC were then harvested by pipetting cells from the Ficoll/serum interface and washed twice.

Culture of PBMC

PBMC (3×10^6 cells/mL) were transferred into 24-well plates in RPMI 1640 (EuroClone, West York, UK) containing 2 *n*-glutamine and 5% foetal calf serum (Hyclone Laboratories Inc, Logan, UT, USA). After 24 h incubation, the supernatants were collected, centrifuged at $400 \times g$ for 10 min at 15°C and stored at -80°C until cytokine determination.

Cytokine Measurement

The cytokines spontaneous production (IL12/IL23p40, IL6, IFN γ , IL17, TNF α , IL10 and TGF β) was measured by enzyme-linked immunosorbent assay (ELISA) using commercial kits (R&D Systems, Minneapolis, MN, USA), following manufacturer's instructions. The spontaneous production of cytokines (IL12/IL23p40, IL6, IFN γ , IL17, TNF α , IL10 and TGF β) was measured by ELISA using commercial kits (R&D Systems, Minneapolis, MN, USA), following manufacturer's instructions. The intra- and inter-assay coefficients of variation were 4% and 7% for IL-12/IL23p40, 5% and 5% for IL6, 6% and 5% for IFN γ , 7% and 7% for IL17, 4% and 6% for TNF α , 6% and 5% for IL10 and 5% and 7% for TGF β , respectively. Cytokine concentrations were determined from the regression line for a standard curve generated by using highly purified recombinant cytokines at different concentrations per-

formed contemporaneously with each assay. The standard curve also served as an internal control over the sensitivity and range of each assay. Data were expressed in picograms per millilitre. All samples were assayed in duplicate.

Flow Cytometry

For the detection of pSTAT1, pSTAT3 and T-bet expression, isolated PBMC were washed once in culture medium (Dulbecco) containing FCS and once in phosphate-buffered saline (PBS) and incubated with specific PE-Cy5-conjugated antibody (CD4, CD8, CD14). CD4⁻ PE-Cy5, CD8⁻ PE-Cy5, CD14⁻ PE-Cy5 and isotype controls were purchased from Beckman Coulter (Miami, FL, USA). In addition, anti-pSTAT1(A-2)-PE antibody, anti-pSTAT3 (B-7)-PE antibody and anti-T-bet (4B10)-PE antibody were purchased from Santa Cruz Biotechnology, Santa Cruz, CA, USA.

The PBMC were then fixed with 2% paraformaldehyde for 10 min. Detection of pSTAT-1, pSTAT-3 and T-bet was performed by intracellular flow cytometry. Cells were permeabilized using a commercially available perm/wash kit (BD Biosciences/Pharmingen) and then washed once in culture medium (Dulbecco) containing FCS and once in PBS. Upon permeabilization, 3×10^5 cells were resuspended in 100 μ L of PBS and incubated for 30 min with the specific PE-conjugated antibody. Cells were washed again with PBS and resuspended in PBS for flow cytometry (Beckman Coulter, EPICS XLTM). Each analysis was performed using at least 50,000 cells that were gated in the lymphocyte-monocyte population region, as determined by light scatter properties (forward scatter versus side scatter). To analyse pSTAT1, pSTAT3 and T-bet expression in monocytes, cells were gated in both the monocyte (morphological gate) and CD14⁺ (immunological gate) regions. To analyse the transcription factor expression in lymphocytes (CD4⁺/CD8⁺ T cells), cells were gated in both the lymphocyte and CD4⁺/CD8⁺ regions. Appropriate fluorochrome-conjugated isotype-matched mAbs were used as control for background staining in each flow acquisition.

Statistical Analysis

Differences in variables between groups were tested by analysis of variance. Post hoc tests were done by using Fisher's protected least significant difference. Results are expressed as mean \pm SD. A *p* level <0.05 was considered to be statistically significant. Correlation was estimated by Spearman rank correlation. Correlation was considered at a *p* value <0.05. Group comparisons (in Table 1) were performed by the Student's *t* test, and *p* <0.05 was taken as significant.

Table 1 Demographic, clinical and MRI features of FSHD patients and healthy subjects included in the study

All data are mean \pm SD. Group comparisons were performed by the Student's *t* test and $p < 0.05$ was taken as significant

CSS Clinical Severity Scale, MRI magnetic resonance imaging, N/A not applicable

* $p = 0.0121$; ** $p = 0.0116$; *** $p = 0.0001$

	FSHD patients		Controls
	Inflammation	No inflammation	
Number	14	11	15
Age (years)	34.5 \pm 11.7*	46.8 \pm 12.9*	37.1 \pm 9.4
Gender (M/F)	7/7	6/5	8/7
Allele fragment size (kb)	21.3 \pm 5.2	18.9 \pm 6.6	N/A
CSS score	3.4 \pm 0.9**	4.2 \pm 0.5**	N/A
MRI-T1 score	74.2 \pm 45.1***	150.9 \pm 36.3***	N/A
MRI-T2 score	12.7 \pm 8.1	N/A	N/A

Results

Patients

Twenty-five consecutive FSHD patients and 15 healthy subjects were included in the immunological study. In FSHD patients, as expected, T1 MRI score highly correlated with CSS ($r = 0.83$; $p < 0.0001$; Fig. 1). On the basis of the T2-STIR-MRI score, 11 patients were assigned to group 1 and 14 patients to group 2 since they showed hyperintensity features in one or more muscles. Muscles that showed a complete fatty-fibrous substitution on T1-W sequences (score 4) did not show hyperintensity features on T2-STIR sequences. Conversely, muscles showing hyperintensity features on T2-STIR sequences turned out to be, on T1-W sequences, either normal (score 0) or partially replaced by fatty-fibrous tissue (scores 1 to 3). Group 1 patients were older ($p = 0.0121$) and showed CSS scores significantly higher than group 2 patients ($p = 0.0116$). No difference was observed in the pathogenic 4q35 EcoRI allele fragment size between the two groups. All these data are summarised in Table 1.

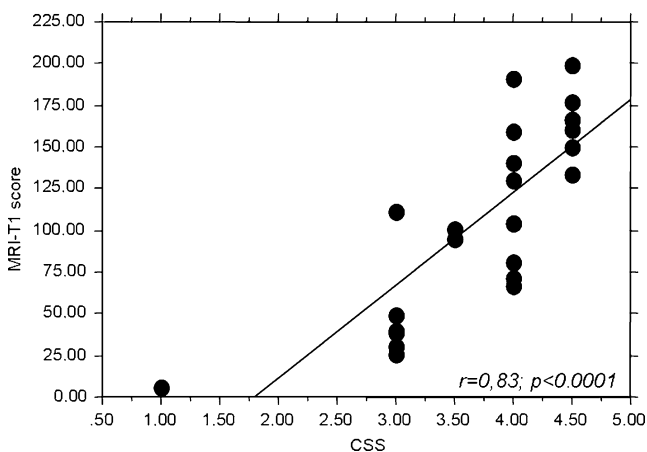


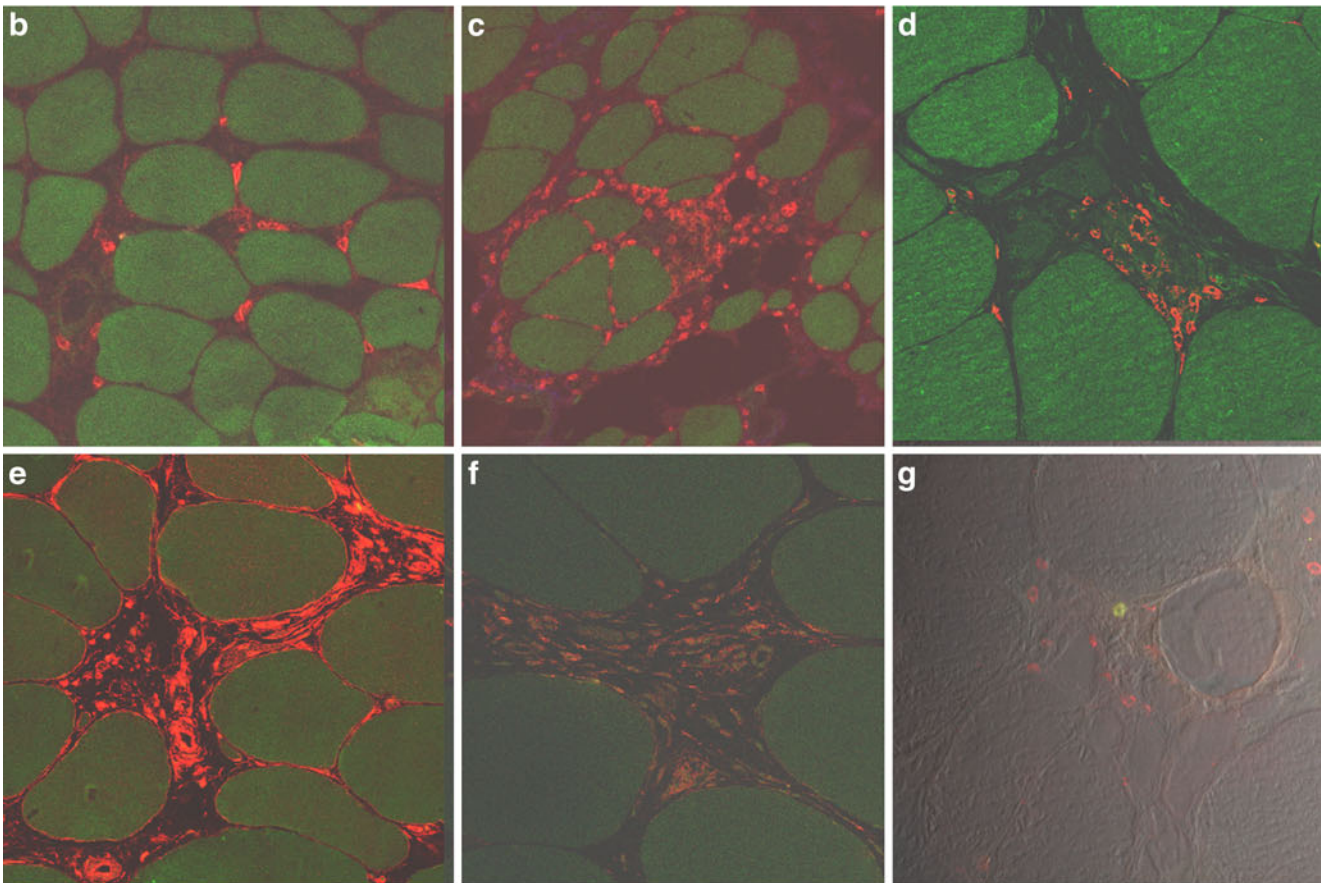
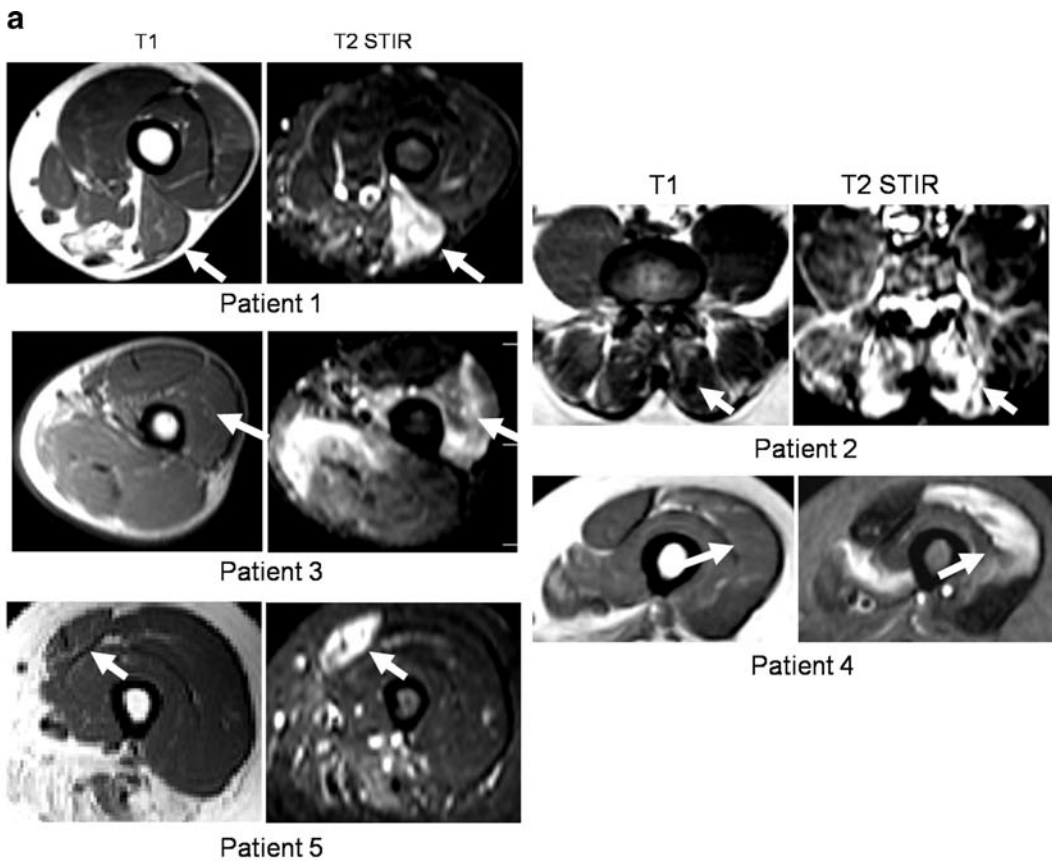
Fig. 1 Correlation between CSS and the MRI T1 score in FSHD patients. A strong significant correlation was found between T1-MRI and CSS scores in FSHD patients. p and r values (Spearman correlation test) are indicated in the figure

Inflammatory Infiltrates on Muscle Biopsies

We analysed muscle specimens from ten different FSHD patients. In five patients, the biopsy was performed in muscles which at MRI were hyperintense on T2 STIR-W images and showed mild or no alterations on T1-W images (Fig. 2a). These were one biceps femoris (sample 1), one vastus medialis (sample 2) and three needle muscle biopsies, two from vastus lateralis (sample 3 and 4) and one from rectus femoris muscles (sample 5). Endomysial connective tissue was found normal or mildly increased. We found endomysial infiltrates, in which CD8⁺ cells predominated (Fig. 2b–d), and perivascular infiltrates, mainly constituted by CD4⁺ cells (Fig. 2f) in all samples. Some muscle fibres in contiguity with endomysial infiltrates expressed low to high levels of HLA ABC (MHC class I) on sarcoplasmic membrane (Fig. 2e). A variable number of CD68-positive cells were present in all samples and predominating in sample 2, in which multiple areas of myophagia were also present. We did not find evidence of partial invasion of non-necrotic muscle fibres by CD8⁺ T cells and presence of B cells or evidence of complement deposition on non-necrotic fibre membranes or on muscle capillaries. Some CD8⁺ cells were also positive for perforin (Fig. 2g).

The infiltrate extension varied among the samples: While numerous and large perivascular and endomysial infiltrates were present in samples 1 and 2, thus closely

Fig. 2 Lower limb muscle MRI and immunohistochemistry study the five patients with T2-STIR hyperintensities. **a** Lower limb muscle MRIs of the five patients with T2-STIR hyperintensities. Arrows indicate sites where muscle biopsy was performed. **b, c** patient 1: CD8⁺ cells (red) predominate in small or large endomysial infiltrates, sometimes completely surrounding apparently non-necrotic fibres. **d** Patient 2: CD8⁺ cells (red) are present in an active myophagia. **e** Patient 5: MHC class I sarcolemmal expression (red) next to an area with both perivascular and endomysial inflammation. In all images, muscle fibres are counterstained with FITC-conjugated phalloidin. **f** Patient 5: perivascular infiltrate mainly composed by CD4⁺ cells. **g** Patient 1: merged Nomarski image of fluorescent double labelling for CD8 (red) and perforin (green) showing a perforin-positive CD8⁺ cell (yellow) nearby an intact muscle fibre



resembling the histopathological features of an inflammatory myopathy, samples 3–5 showed predominantly small- or medium-sized endomysial infiltrates. Sample 5 also showed interstitial oedema and slightly enlarged vessels. FSHD needle muscle biopsies obtained from five normal appearing muscles (on both T1 and T2-STIR sequences) were normal or displayed only mild myopathic changes with routine histological and histochemical stainings, and no inflammatory features were evident on them.

pSTAT1, pSTAT3 and T-bet in Circulating CD4⁺, CD8⁺ T Cells and Monocytes from FSHD Patients and Controls

A higher percentage of CD14⁺T-bet⁺ cells was observed in patients than in healthy subjects; otherwise, no differences were found in the percentages of CD4⁺T-bet⁺, CD8⁺T-bet⁺ T cells between patients and controls (Fig. 3a). The percentages of circulating CD4⁺pSTAT1⁺, CD8⁺pSTAT1⁺ and CD14⁺pSTAT1⁺ cells were higher in FSHD patients than in controls, however without reaching statistical significant values (Fig. 3b). No difference was found in the percentages of CD4⁺pSTAT3⁺, CD8⁺pSTAT3⁺ and CD14⁺pSTAT3⁺ cells between FSHD patients and controls (Fig. 3c). When we separately analysed the two groups of FSHD patients, we found higher percentages of CD8⁺pSTAT1⁺, CD8⁺T-bet⁺, CD14⁺pSTAT1⁺ and CD14⁺T-bet⁺ cells in peripheral blood of group 2 than both group 1 and healthy subjects (Fig. 3d, e). The percentage of CD14⁺pSTAT3⁺ cells was significantly higher in group 2 than in controls and in group 1 than in controls without reaching significant values, while there was no difference in the percentage of CD14⁺pSTAT3⁺ cells between group 1 and group 2 (Fig. 3f). On the contrary, no difference was found in the percentages of CD4⁺pSTAT1⁺, CD4⁺pSTAT3⁺, CD4⁺T-bet⁺ and CD8⁺pSTAT3⁺ cells among the different study groups (Fig. 3d–f). Representative two-parameter plots of T-bet, pSTAT1 and pSTAT3 in CD4⁺, CD8⁺ T cells and monocytes are described in Fig. 4.

When we compared the immunological findings with muscle MRI features, we found that the percentages of CD8⁺pSTAT1⁺ (Fig. 5b), CD14⁺pSTAT1⁺ (Fig. 5b) and CD8⁺T-bet⁺ cells (Fig. 5a) significantly correlated with the number of T2-STIR hyperintense muscles. Otherwise, we did not find any correlation between pSTAT1⁺, pSTAT3⁺ and T-bet⁺ cells and the degree of muscle fatty-fibrous replacement as defined by the T1 MRI score. Accordingly, we did not find any correlation between pSTAT1⁺, pSTAT3⁺ and T-bet⁺ cells and CSS score (data not shown).

Cytokine Production by PBMC from FSHD Patients and Controls

We found higher IFN γ , TNF α , IL12/IL23p40, IL6 and IL10 levels in FSHD patients than in controls (Fig. 6a–c, e, f),

while no differences were observed in IL17 and TGF β levels (Fig. 6d, g). When we divided FSHD patients into two groups according to different MRI features (T2-STIR-MRI score), we observed that FSHD patients with MRI features of inflammation (group 2) showed significant higher IFN γ , TNF α and IL12/IL23p40 levels than both FSHD patients without MRI features of inflammation (group 1) and healthy subjects (Fig. 6a–c). IL6 and IL10 production by PBMC was higher in group 2 than in group 1 while both groups of FSHD patients showed higher IL6 and IL10 levels than healthy subjects (Fig. 6e, f). Otherwise, no significant difference was observed in IL17 and TGF β levels between the two groups of FSHD patients as well as between each FSHD group and the control group (Fig. 6d, g). No correlations were found between cytokine production by PBMC from FSHD patients and muscle MRI features or CSS score (data not shown).

Discussion

In this study, we performed ten muscle biopsies driven by MRI study in FSHD patients and found that inflammatory changes appear to be a constant finding when samples are obtained from muscles showing hyperintensity features on T2-STIR sequences but not from normal appearing ones. These data indicate that T2-STIR abnormalities in muscles from FSHD patients are correlated with inflammation, and therefore, in the following part of this discussion, we will indifferently use the terms inflammation and hyperintensity features for these findings.

Our pathological results, in particular the composition of both perivascular and endomysial infiltrates, are similar to those previously reported by others [10–12] and consistent with a significant presence of CD8⁺ T cells in the endomysium close to non-necrotic fibres. CD8⁺ T cells also invade rare degenerating fibres, together with macrophages. No histopathological data support a complement-mediated damage against muscle vessels or fibres, differently from dermatomyositis or dysferlinopathies [22]. As described by Arahata and colleagues, neither did we discover evidence of partial invasion of non-necrotic muscle fibres by CD8⁺ T cells, but a cytotoxic action of these cells cannot be excluded only on the basis of this finding. To this regard, we must underline the presence of focal (limited to single fibres or portions of the sarcolemma) expression of MHC class I in our samples and the expression of perforin in scattered CD8⁺ T cells that we report for the first time in FSHD muscle biopsies.

To better define the contribution of inflammation to the pathophysiology of FSHD, we evaluated in the peripheral blood of FSHD patients and controls the percentages of T-bet-, pSTAT1- and pSTAT3-positive

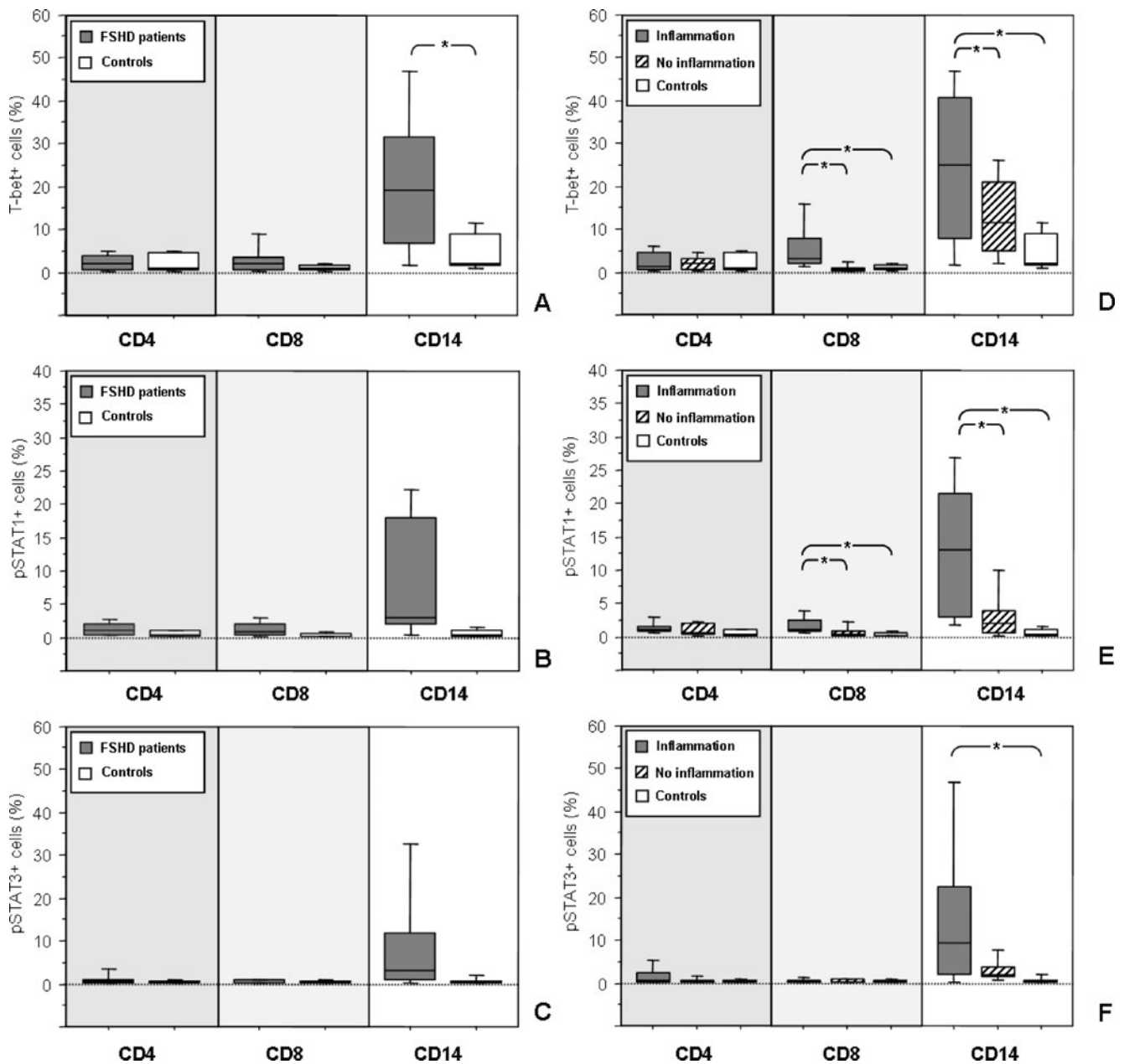
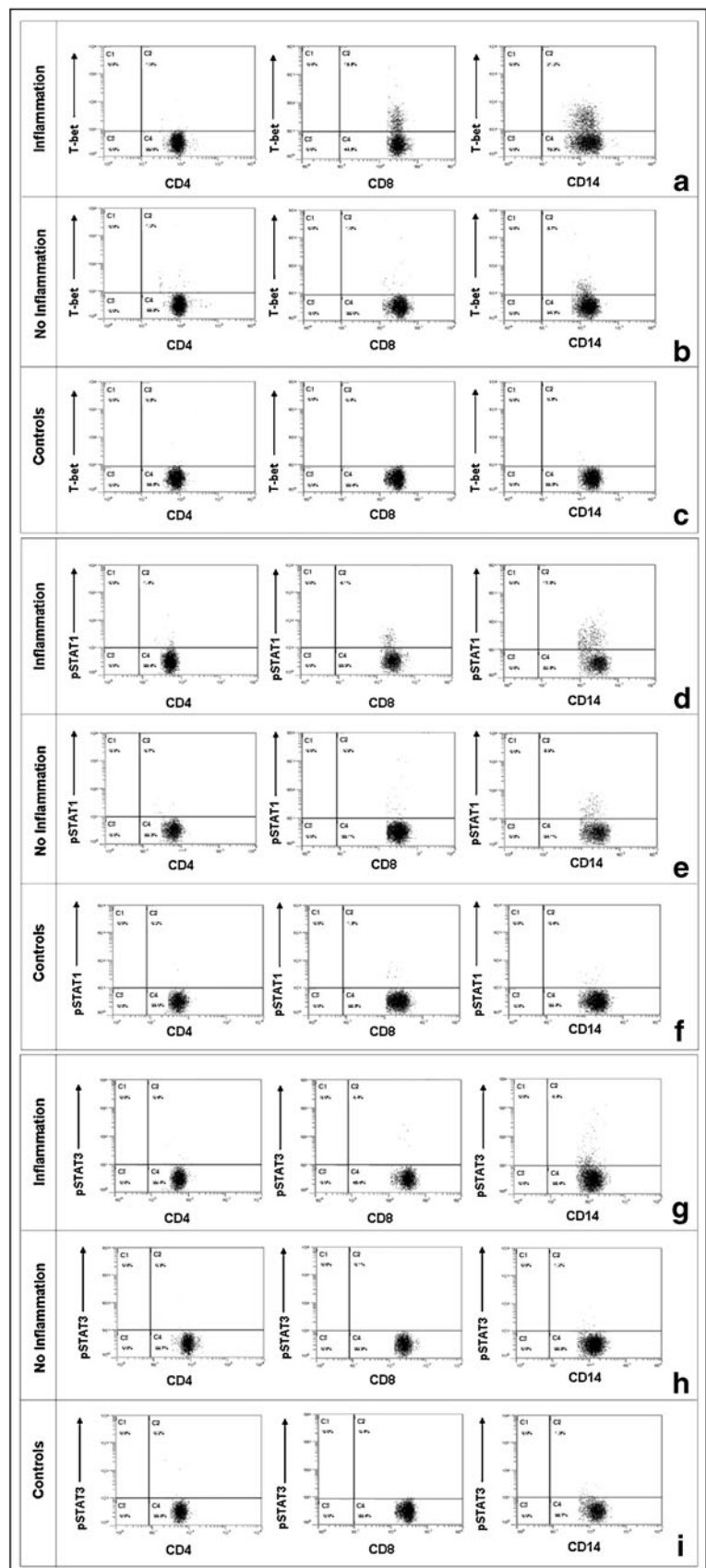


Fig. 3 Percentage of T-bet⁺, pSTAT1⁺, pSTAT3⁺ T cells and monocytes in FSHD patients with and without inflammatory pattern at lower limb muscle MRI and in healthy subjects. **a** A higher percentage of circulating CD14⁺T-bet⁺ cells was observed in FSHD patients than in controls (**a**, $p=0.0034$). No difference was found in CD4⁺T-bet⁺ and CD8⁺T-bet⁺ T cell percentages between FSHD patients and healthy subjects. **b**, **c** No difference was observed in the percentages of pSTAT1⁺ and pSTAT3⁺ T cells and monocytes between FSHD patients and controls. **d** The percentages of CD8⁺T-bet⁺ T cells and CD14⁺ T-bet⁺ cells were significantly higher in FSHD patients with inflammatory pattern at lower limb MRI than in patients without inflammatory signs and controls ($p=0.0250$ and $p=0.0141$, respectively, for CD8⁺ and $p=0.0058$ and $p<0.0001$, respectively, for CD14⁺ cells). **e** The percentages of CD8⁺pSTAT1⁺ T cells and CD14⁺pSTAT1⁺ cells were significantly higher in FSHD patients with inflammatory pattern at lower limb MRI than in patients without

inflammatory signs and controls ($p=0.0278$ and $p=0.0231$, respectively, for CD8⁺ and $p=0.0016$ and $p=0.0011$, respectively, for CD14⁺ cells). **f** The percentage of CD14⁺pSTAT3⁺ cells was significantly higher in FSHD patients with inflammatory pattern than in controls. No differences were observed between FSHD patients without and with inflammatory signs and between FSHD patients without inflammatory signs and controls. No differences in the percentages of CD4⁺pSTAT3⁺ and CD8⁺pSTAT3⁺ T cells were found among FSHD patients with and without inflammatory pattern at muscle MRI and controls. Box plots express the first (Q1) and third (Q3) quartiles within a given dataset by the upper and lower horizontal lines in a rectangular box, in which there is a horizontal line showing the median. The whiskers extend upwards and downwards to the highest or lowest observation within the upper (Q3+1.5×interquartile range) and lower (Q1–1.5×interquartile range) limits. p values indicate statistical significances (<0.05) between the different groups

Fig. 4 Representative two-parameter plots represent only cells gated on the lymphocyte populations (CD4 or CD8 staining) and monocyte populations (CD14 staining). The y-axis of each histogram represents specific fluorescence of T-bet-PE, pSTAT1-PE and pSTAT3-PE; the x-axis represents specific fluorescence of extracellular CD4-PE-Cy5, CD8-PE-Cy5, CD19 (T lymphocytes) and CD14-PE-Cy5 (monocytes) on four-decade logarithmic scales. These representative two-parameter plots are obtained from one FSHD patient with inflammation at muscle MRI, from one FSHD patient without MRI inflammation and from one control. Quadrants were set using appropriate isotype controls for each intra- and extracellular antibody



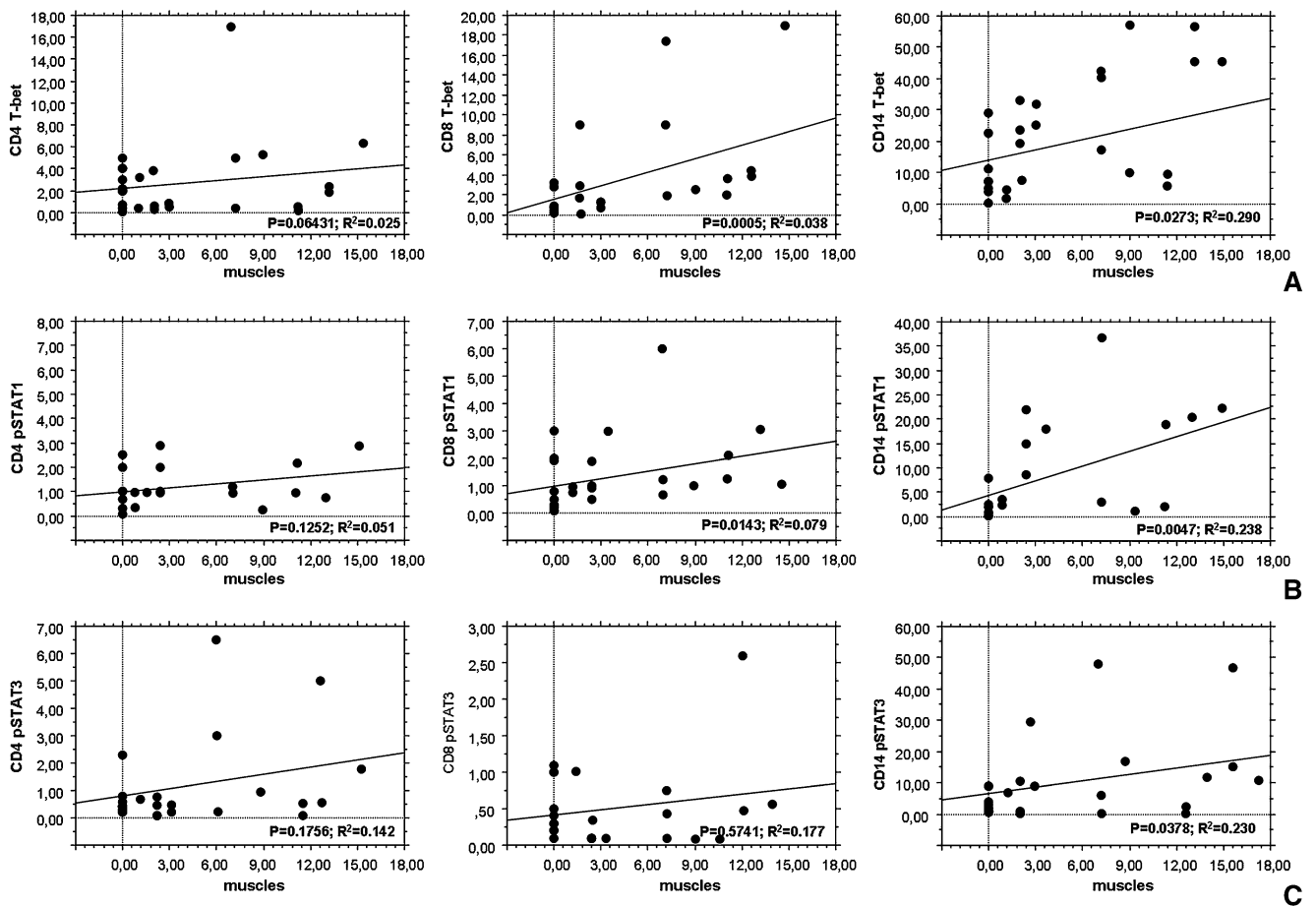


Fig. 5 Correlation between the percentages of T-bet, pSTAT1 and pSTAT3 positive CD4⁺, CD8⁺ T cells and CD14⁺ cells and the number of T2-STIR-positive muscles at MRI in FSHD patients. A significant correlation was found between the value of MRI T2 score

and the percentages of T-bet⁺ and pSTAT1⁺ CD8⁺ T cells. A significant correlation was also observed between the value of MRI T2 score and the percentage of pSTAT1⁺ monocytes. *p* and *R*² value (Spearman correlation test) are indicated in the figure

cells and the production of several pro-inflammatory and anti-inflammatory cytokines by mononuclear cells. T-bet is a specific transcription factor that seems to play a central role in type 1 immunity by influencing genetic programme in both innate and adaptive immunity [23]. T-bet is mainly induced by IFN γ , through STAT1 activation [24, 25], and, once expressed, amplifies IFN- γ production by T cells, NK cells, monocytes and dendritic cells [26]. Also IL12, by STAT4 activation, can induce T-bet expression and increase IFN γ production by T cells [27]. Activated CD8⁺ T cells produce TNF α and IFN γ , and T-bet is critical for IFN γ in vivo production by CD8⁺ T cells [28]. T-bet is also required for CD8⁺ T cell full effector function [29] and perforin and granzyme B expression [30].

FSHD patients showed an increased percentage of circulating CD14⁺T-bet⁺ cells and an increased spontaneous production of IL12/IL23p40, IFN γ , TNF α , IL6 and IL10 by PBMC in comparison to controls, while no difference

was observed in TGF β and IL17 levels. When we divided FSHD patients in two groups on the basis of MRI features, we found an increased production of IL12/IL23p40, IFN γ and TNF α by PBMC and higher percentages of CD8⁺pSTAT1⁺, CD8⁺T-bet⁺, CD14⁺pSTAT1⁺ and CD14⁺T-bet⁺ cells in the peripheral blood from group 2 patients, displaying inflammatory features on MRI examination than both group 1 patients, not displaying MRI evidence of inflammation, and healthy subjects. The percentages of CD8⁺pSTAT1⁺, CD8⁺T-bet⁺ and CD14⁺pSTAT1⁺ cells positively correlated with the number of muscles showing hyperintensity features at MRI T2-STIR sequences but not with T1 MRI and CSS scores, indicating that only the active phase of inflammation is associated with peripheral blood immune cell activation, which is conversely absent when MRI examination displays merely irreversible fatty-fibrous replacement of muscle tissue. On the contrary, CSS, as an index of disease

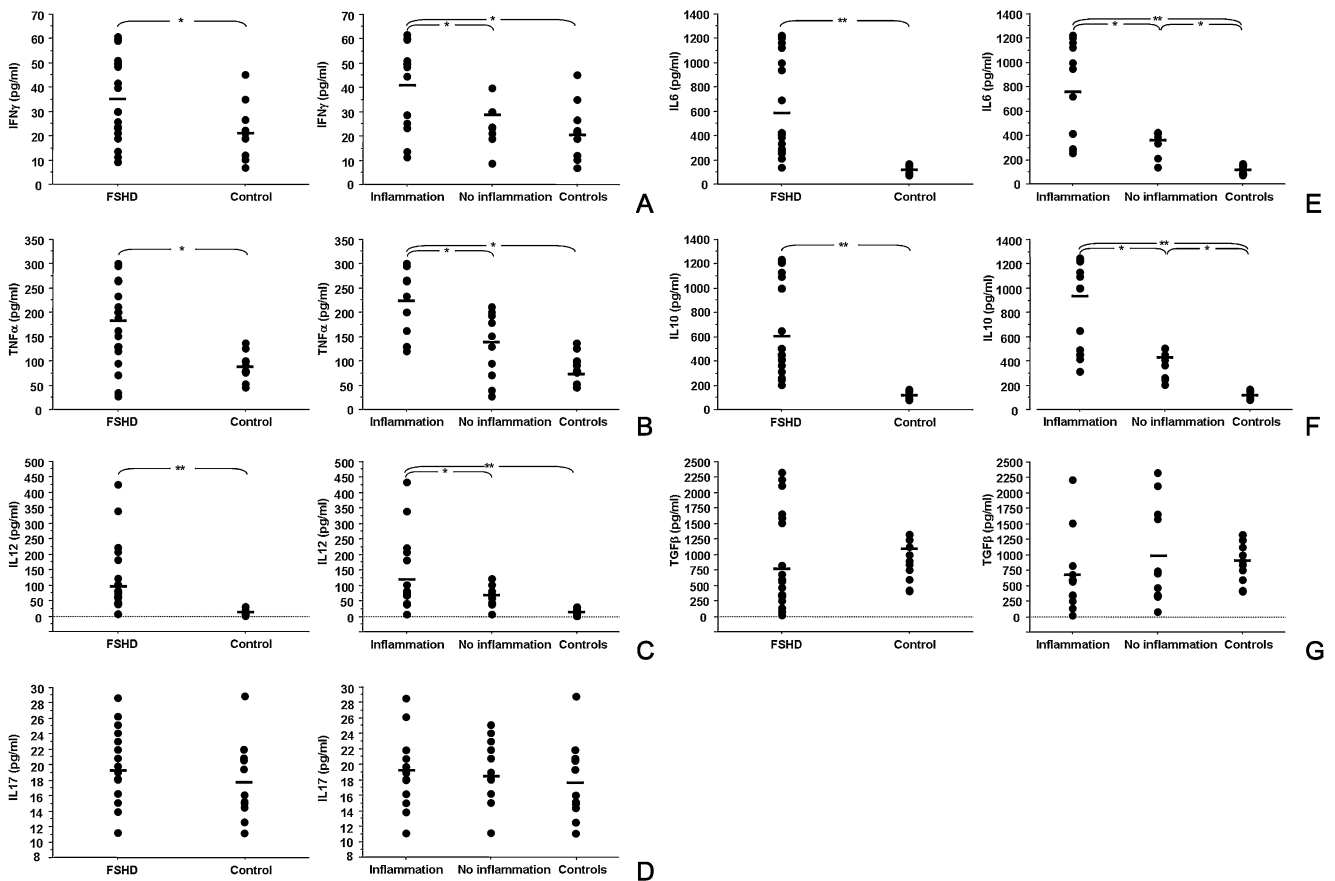


Fig. 6 Cytokine spontaneous production by PBMC from FSHD patients with inflammation at muscle MRI, FSHD patients without inflammation at muscle MRI and healthy subjects. Higher IFN γ (a), TNF α (b), IL12/IL23p40 (c), IL6 (e) and IL10 (f) levels were observed in FSHD patients than in controls ($p=0.0402$, $p=0.0011$, $p=0.0010$, $p=0.0005$ and $p=0.0001$, respectively). Significant higher IFN γ (a), TNF α (b), IL12/IL23p40 (c), IL6 (e) and IL10 (f) levels were observed in FSHD patients with MRI features of inflammation

than both FSHD patients without MRI features of inflammation ($p=0.0181$, $p=0.0049$, $p=0.0415$, $p=0.0032$ and $p=0.0003$, respectively) and healthy subjects ($p=0.0041$, $p<0.0001$, $p=0.0020$, $p<0.0001$ and $p=0.0020$, respectively). Moreover, IL6 (e) and IL10 (f) production by PBMC was higher in FSHD patients without MRI inflammation than healthy subjects ($p=0.0422$ and $p=0.0405$, respectively). P value indicates statistical differences (<0.05) between the different groups

severity, is related to irreversible lesions due to fatty-fibrous replacement of muscle tissue, which are detected by T1-W sequences and are not hyperintense on T2-STIR sequences. All these data, in addition with the presence of perforin expressing CD8⁺ T cells in muscle infiltrates, indicate an activation of immune cells, mainly CD8⁺ T cells, producing pro-inflammatory cytokines such as IFN γ , TNF α and IL12/IL23p40 in FSHD patients showing inflammatory features at muscle MRI but not in FSHD patients showing only T1-W abnormalities and controls. The younger age of patients with inflammatory features at muscle MRI suggests that the immune process is mainly present in the early phase of disease. Hyperintensity features at MRI T2-STIR sequences may be observed in muscles partially replaced by fat but also in muscles normally appearing on T1-W sequences. The last condition is the case of five muscles we chose to perform muscle biopsy. The

absence of important fatty-fibrous replacement on both MRI and pathological examinations suggests that in single muscles, inflammation may be an early event in the pathophysiological cascade underlying the dystrophic process.

Both groups of FSHD patients showed higher spontaneous PBMC production of IL6 and IL10 than controls, group 2 showing a higher production than group 1. Both IL6 and IL10 act through pSTAT3 activation. IL6-mediated STAT3 activation favours monocytic differentiation [31], augments T cell proliferation through the suppression of apoptosis [32] and, in presence of TGF β and IL23, favours the differentiation of Th17 cells [33, 34]. IL10 is a cytokine with broad anti-inflammatory properties and has a key effect on the suppression of Th1 cell responses [35]. IL10-mediated-STAT3 signalling can inhibit dendritic cell maturation from monocytes [36], inflammatory cytokine secretion such that of IL12 [37],

MHC class II and costimulatory molecule expression by both macrophages and dendritic cells [38, 39]. Additionally, IL6-mediated STAT3 activation can induce IL10 production in Th1, Th2 and Th17 T cells to temper inflammatory response [40]. We found similar percentages of CD14⁺pSTAT3⁺ cells in the two groups of patients and an increased percentage of these cells in group 2 than in control group whereas there was no difference in the percentage of CD4⁺pSTAT3⁺ and CD8⁺pSTAT3⁺ T cells among the three groups.

These data suggest that in FSHD patients, IL6 and IL10 are produced mainly by monocytes. The production of IL6 by monocytes may favour CD8⁺ T cell activation and increase their proliferation and effector functions. Conversely, IL10 may be produced by monocytes as a way of preventing excessive inflammation and immunity.

However, it is worth noting that an augmented production of IL6 and IL10 by PBMC as compared to controls was present in both groups of FSHD patients. IL6 causes skeletal muscle atrophy in rats [41, 42] and correlates with muscle mass and strength loss in humans [43, 44] whereas endogenous IL10 attenuates IL6 expression by skeletal muscles following an inflammatory insult [45]. In this context, we can hypothesize that in all FSHD patients, IL6 produced by monocytes and muscles is only partially inhibited by IL10 produced by monocytes favouring, even when episodes of acute/subacute inflammation are overcome, diffuse muscle atrophy.

Conclusions

In conclusion, our data demonstrate that the areas of hyperintensity on T2-STIR images at muscle MRI in FSHD patients are characterized by the presence of inflammatory infiltrates mainly composed by CD8⁺ in the endomysium. Moreover, we showed, in peripheral blood of FSHD patients with hyperintensity features at MRI T2-STIR sequences, the presence of activated immune cells, mainly CD8⁺ T cells. Therefore, inflammation, as an early event in single muscle involvement, may play a role in FSHD pathophysiology by promoting muscle pathology and favouring disease progression and might constitute a potential target for the treatment of the disease.

Further studies are necessary to demonstrate whether CD8⁺ T cell activation observed in muscles and peripheral blood from FSHD patients is generated by muscle degeneration as a bystander phenomenon or may be caused by transcriptional dysregulation of multiple genes involved in the autoimmune response.

Acknowledgements We thank Manuela Papacci and Teresa Maresca for technical assistance.

References

- Steinman L. Four easy pieces: interconnections between tissue injury, intermediary metabolism, autoimmunity, and chronic degeneration. *Proc Am Thorac Soc.* 2006;3:484–6.
- Spencer MJ, Tidball JG. Do immune cells promote the pathology of dystrophin-deficient myopathies. *Neuromuscul Disord.* 2001;11:556–64.
- Moser H, Dubye P, Fatemi A. Progress in X-linked adrenoleukodystrophy. *Curr Opin Neurol.* 2004;17:263–9.
- Ranes J, Stoller K. Review of alpha 1-antitrypsin deficiency. *Semin Respir Crit Care Med.* 2005;26:154–66.
- Pescatori M, Broccolini A, Minetti C, Bertini E, Bruno C, D'amico A, et al. Gene expression profiling in the early phases of DMD: a constant molecular signature characterizes DMD muscle from early postnatal life throughout disease progression. *FASEB J.* 2007;21:1210–26.
- Nagaraju K, Rawat R, Veszelovszky E, Thapliyal R, Kesari A, Sparks S, et al. Dysferlin deficiency enhances monocyte phagocytosis: a model for the inflammatory onset of limb-girdle muscular dystrophy 2B. *Am J Pathol.* 2008;172:774–85.
- van Deutekom JC, Wijmenga C, van Tienhoven EA, Gruter AM, Hewitt JE, Padberg GW, et al. FSHD associated DNA rearrangements are due to deletions of integral copies of a 3.2 kb tandemly repeated unit. *Hum Mol Genet.* 1993;2:2037–42.
- Tawil R, Van Der Maarel SM. Facioscapulohumeral muscular dystrophy. *Muscle Nerve.* 2006;34:1–15.
- Tupler R, Perini G, Pellegrino MA, Green MR. Profound misregulation of muscle-specific gene expression in facioscapulohumeral muscular dystrophy. *Proc Natl Acad Sci USA.* 1999;96:12650–4.
- Munsat TL, Piper D, Cancilla P, Mednick J. Inflammatory myopathy with facioscapulohumeral distribution. *Neurology.* 1972;22:335–47.
- Figarella-Branger D, Pellissier JF, Serratrice G, Pouget J, Bianco N. Immunocytochemical study of the inflammatory forms of facioscapulohumeral myopathies and correlation with other types of myositis. *Ann Pathol.* 1989;9:100–8.
- Arahata K, Ishihara T, Fukunaga H, Orimo S, Lee JH, Goto K, et al. Inflammatory response in facioscapulohumeral muscular dystrophy (FSHD): immunocytochemical and genetic analyses. *Muscle Nerve.* 1995;2:S56–66.
- Tawil R, McDermott MP, Pandya S, King W, Kissel J, Mendell JR, et al. A pilot trial of prednisone in facioscapulohumeral muscular dystrophy FSH-DY group. *Neurology.* 1997;48:46–9.
- Mercuri E, Talim B, Moghadaszadeh B, Petit N, Brockington M, Counsell S, et al. Clinical and imaging findings in six cases of congenital muscular dystrophy with rigid spine syndrome linked to chromosome 1p (RSMD1). *Neuromuscul Disord.* 2002;12:631–8.
- Sookhoo S, Mackinnon I, Bushby K, Chinnery PF, Birchall D. MRI for the demonstration of subclinical muscle involvement in muscular dystrophy. *Clin Radiol.* 2007;62:160–5.
- Olsen DB, Gideon P, Jeppesen TD, Vissing J. Leg muscle involvement in facioscapulohumeral muscular dystrophy assessed by MRI. *J Neurol.* 2006;253:1437–41.
- Kan HE, Scheenen TW, Wohlgemuth M, Klomp DW, van Loosbroek-Wagenmans I, Padberg GW, et al. Quantitative MR imaging of individual muscle involvement in facioscapulohumeral muscular dystrophy. *Neuromuscul Disord.* 2009;19:357–62.
- May DA, Disler DG, Jones EA, Balkissoon AA, Manaster BJ. Abnormal signal intensity in skeletal muscle at MR imaging: patterns, pearls, and pitfalls. *Radiographics.* 2000;20:S295–315.
- Kamath S, Venkatanarasimha N, Walsh MA, Hughes PM. MRI appearance of muscle denervation. *Skeletal Radiol.* 2008;37:397–404.

20. Ricci E, Galluzzi G, Deidda G, Cacurri S, Colantoni L, Merico B, et al. Progress in the molecular diagnosis of facioscapulohumeral muscular dystrophy and correlation between the number of KpnI repeats at the 4q35 locus and clinical phenotype. *Ann Neurol*. 1999;45:751–7.
21. Lynöe N, Sandlund M, Dahlqvist G, Jacobsson L. Informed consent: study of quality of information given to participants in a clinical trial. *BMJ*. 1991;303:610–3.
22. Brunn A, Schroder R, Deckert M. The inflammatory reaction pattern distinguishes primary dysferlinopathies from idiopathic inflammatory myopathies: an important role for the membrane attack complex. *Acta Neuropathol*. 2006;112:325–32.
23. Wang J, Fathman JW, Lugo-Villarino G, Scimone L, von Andrian U, Dorfman DM, et al. Transcription factor T-bet regulates inflammatory arthritis through its function in dendritic cells. *J Clin Invest*. 2006;116:414–21.
24. Lighvani AA, Frucht DM, Jankovic D, Yamane H, Aliberti J, Hissong BD, et al. T-bet is rapidly induced by interferon-gamma in lymphoid and myeloid cells. *Proc Natl Acad Sci USA*. 2001;98:15137–42.
25. Afkarian M, Sedy JR, Yang J, Jacobson NG, Cereb N, Yang SY, et al. T-bet is a STAT1-induced regulator of IL-12R receptor in naïve CD4+ cells. *Nat Immunol*. 2002;3:549–57.
26. Mullen AC, High FA, Hutchins AS, Lee HW, Villarino AV, Livingston DM, et al. Role of T-bet in commitment of TH1 cells before IL-12-dependent selection. *Science*. 2001;292:1907–10.
27. Yang Y, Ochando JC, Bromberg JS, Ding Y. Identification of a distant T-bet enhancer responsive to IL-12/Stat4 and IFN γ /Stat1 signals. *Blood*. 2007;110:2494–500.
28. Mayer KD, Mohrs K, Reiley W, Wittmer S, Kohlmeier JE, Pearl JE, et al. Cutting edge: T-bet and IL-27R are critical for in vivo IFN-gamma production by CD8 T cells during infection. *J Immunol*. 2008;180:693–7.
29. Sullivan BM, Juedes A, Szabo SJ, von Herrath M, Glimcher LH. Antigen-driven effector CD8 T cell function regulated by T-bet. *Proc Natl Acad Sci USA*. 2003;100:15818–23.
30. Cruz-Guilloty F, Pipkin ME, Djuretic IM, Levanon D, Lotem J, Lichtenheld MG, et al. Runx3 and T-box proteins cooperate to establish the transcriptional program of effector CTLs. *J Exp Med*. 2009;206:51–9.
31. Manel N, Unutmaz D, Littman DR. The differentiation of human T(H)-17 cells requires transforming growth factor-beta and induction of the nuclear receptor ROR γ . *Nat Immunol*. 2008;9:641–9.
32. Takeda K, Kaisho T, Yoshida N, Takeda J, Kishimoto T, Akira S. Stat3 activation is responsible for IL-6-dependent T cell proliferation through preventing apoptosis: generation and characterization of T cell-specific Stat3-deficient mice. *J Immunol*. 1998;161(9):4652–60.
33. Mangan JK, Rane SG, Kang AD, Amanullah A, Wong BC, Reddy EP. Mechanisms associated with IL-6-induced up-regulation of Jak3 and its role in monocytic differentiation. *Blood*. 2004;103:4093–101.
34. Volpe E, Servant N, Zollinger R, Bogiatzi SI, Hupé P, Barillot E, et al. A critical function for transforming growth factor-beta, interleukin 23 and proinflammatory cytokines in driving and modulating human T(H)-17 responses. *Nat Immunol*. 2008;9:650–7.
35. O'Garra A, Vieira P. T(H)1 cells control themselves by producing interleukin-10. *Nat Rev Immunol*. 2007;7:425–8.
36. Corinti S, Albanesi C, la Sala A, Pastore S, Girolomoni G. Regulatory activity of autocrine IL-10 on dendritic cell functions. *J Immunol*. 2001;166:4312–8.
37. Hoentjen F, Sartor RB, Ozaki M, Jobin C. STAT3 regulates NF-kappaB recruitment to the IL-12p40 promoter in dendritic cells. *Blood*. 2005;105:689–96.
38. Williams L, Bradley L, Smith A, Foxwell B. Signal transducer and activator of transcription 3 is the dominant mediator of the anti-inflammatory effects of IL-10 in human macrophages. *J Immunol*. 2004;172:567–76.
39. Murray PJ. Understanding and exploiting the endogenous interleukin-10/STAT3-mediated anti-inflammatory response. *Curr Opin Pharmacol*. 2006;6:379–86.
40. Stumhofer JS, Silver JS, Laurence A, Porrett PM, Harris TH, Turka LA, et al. Interleukins 27 and 6 induce STAT3-mediated T cell production of interleukin 10. *Nat Immunol*. 2007;8:1363–71.
41. Janssen SP, Gayan-Ramirez G, Van den Bergh A, Herijgers P, Maes K, Verbeken E, et al. Interleukin-6 causes myocardial failure and skeletal muscle atrophy in rats. *Circulation*. 2005;111:996–1005.
42. Haddad F, Zaldivar F, Cooper DM, Adams GR. IL-6-induced skeletal muscle atrophy. *J Appl Physiol*. 2005;98:911–7.
43. Schaap LA, Pluijm SM, Deeg DJ, Visser M. Inflammatory markers and loss of muscle mass (sarcopenia) and strength. *Am J Med*. 2006;119:9–17.
44. Toth MJ, Ades PA, Tischler MD, Tracy RP, LeWinter MM. Immune activation is associated with reduced skeletal muscle mass and physical function in chronic heart failure. *Int J Cardiol*. 2006;109:179–87.
45. Huey KA, McCusker RH, Kelley KW. Exaggerated expression of skeletal muscle-derived interleukin-6, but not TNF α , in mice lacking interleukin-10. *J Neuroimmunol*. 2008;199:56–62.